DISORDER EFFECTS IN SUPERCONDUCTORS

DISORDER EFFECTS ON AC FLUCTUATION CONDUCTIVITY IN HIGH-T_c SUPERCONDUCTORS

By

BO ZHOU, B.Sc.Hons.

A Thesis
Submitted to the School of Graduate Studies
in Partial Fulfilment of the Requirements
for the Degree
Master of Science

McMaster University

MASTER OF SCIENCE (2005) McMaster University
(Condensed Matter) Hamilton, Ontario

TITLE: DISORDER EFFECTS ON AC FLUCTUATION CONDUCTIVITY IN HIGH-T_c SUPERCONDUCTORS

AUTHOR: Bo Zhou,B.Sc.Hons.(Peking University)

SUPERVISOR: Dr. C. Kallin, Dr. A.J. Berlinsky

NUMBER OF PAGES: viii, 48

Abstract

For High-T_c superconductors the fluctuation regime is much wider than conventional superconductors due to the short coherence length and high transition temperature. AC measurements can probe the conductivity at a wide range of frequencies, and therefore provide a test of the scaling properties predicted from theory. The measured critical exponents and width of the fluctuation peak are sample dependent, which suggests that the sample imhomogeneities may play an important role in the critical region.

In this thesis we study the effects of disorder on the fluctuation conductivity in the critical regime of zero-field normal-superconducting transition by the time-dependent Ginzburg-Landau theory. We set up a discretized model of the superconductor and calculate the two-dimensional and three-dimensional scaling function without disorder above T_c. The result of the discretized model deviates slightly from previous theoretical studies of the continuous model, which can be explained by a finite short-wavelength cutoff in Ginzburg-Landau theory. Our results agree well with other theoretical investigations on cutoff effects from an analytical approach.

Disorder in a superconductor is modeled by a distribution of T_c's at the lattice

sites. We add random disorder to a two-dimensional lattice and calculate the scaling functions averaged over 1000 disorder configurations. When disorder is weak, the scaling functions are increased when T is close T_c. At strong disorder anomalous behavior may occur at the region close to T_c.

Contents

List of Figures

Acknowledgements

Thanks to my supervisor, Dr. A. J. Berlinsky and Dr. C. Kallin, for suggesting this project. During the last two years, they provided advice, patience, encouragement, and lots of good ideas. I am impressed by their enthusiasm in research and insight into the area we are working in. It is hard to overestimate the value of their instructions on the essential factors of scientific research, including not only many useful techniques in calculation but also bibliography reading, presenting in public and communicating with persons in the same profession.

I am also indebted to many other people in this department. Dr. E. Sorensen, who discussed with me this project and offered suggestions on numerical work; Dr. Rastko Sknepnek, who cooperated with me at an early step and helped me on integration; Fei Lin, who answered lots of my questions and shared his experience about Fortran 90 programming. I also appreciate him for providing me the LaTeX documentations. Special thanks to Suyan Li, who worked with me in the same office under the noise of my computer while running programs.

A final thanks to my parents, for their love and support all along.

Chapter 1

Introduction

1.1 AC Fluctuation Conductivity

1.1.1 DC and AC Conductivity in Superconductors

A superconductor is characterized by its zero resistivity, or infinite conductivity for a DC current. However, there will be nonzero dissipation at any finite frequency since the electrons will be accelarated and decelerated by the oscillating electric field. In a general two fluid model, the linear response of the normal and superconducting electrons ($i = n, s$) to a field $Ee^{i\omega t}$ are: [3]

$$\sigma_i(\omega) \equiv \sigma_{1i}(\omega) - i\sigma_{2i}(\omega) = (n_i e^2 \tau_i/m)/(1 + i\omega\tau_i). \tag{1.1}$$

If τ_s is infinite, σ_{1s} becomes a delta function, and the imaginary part, σ_{2s}, is $n_s e^2/m\omega$, which is the result of the first London equation.

1.1.2 Fluctuation Effects

Thermodynamic fluctuations near superconducting phase transitions have been studied for several decades. In the vicinity of T_c, fluctuation induced behavior occurs in many physical quantities, such as the specific heat, the diamagnetic susceptibility, the DC and AC electritical conductivity. These effects can be observed in various experiments. Theoretically, the phenomenological Ginzburg-Landau theory provides a foundation for understanding the effects of fluctuation. A review in this area was made by W. J. Skocpol and M. Tinkham in 1975 [4].

Above T_c fluctuations will create superconducting regions and produce the excess conductivity called the "paraconductivity". For the dynamical conductivity, the time-dependent Ginzburg-Landau equation determines the equation of motion for the order-parameter which describes these superconducting regions. By calculating fluctuation effects about mean field theory, Schmidt obtained the Aslamazov-Larkin term of the frequency-dependent conductivity for bulk materials, thin films and thin wires above T_c [5] in 1968 and below T_c [6] in 1969.

In conventional low-T_c superconductors, fluctuation effects are generally quite small because of the long correlation length. As a result it is hard to observe fluctuations beyond the Gaussian (mean field) level experimentally. After the discovery of high-T_c superconductors, there has been a resurgence of interest in fluctuation effects both theoretically and experimentally. Due to the high temperature and short correlation length, fluctuations in high-T_c materials are greatly enhanced. The critical

region near T_c is therefore much wider and can be probed experimentally. According to a qualitative estimation based on the Ginzburg criterion, the width of the critical region in high-T_c superconductors is of the order Kelvins, whereas in low-T_c superconductors it is at most 10^{-6}K.

1.2 Microwave Measurements

The microwave cavity perturbation method [7] is a technique to probe the complex conductivity at microwave frequencies. The measurable quantity is the complex surface impedance $Z_s \equiv R_s + iX_s$, which is related to the complex conductivity via:

$$Z_s(\omega) = \left(\frac{i\mu_0\omega}{\sigma_1 - i\sigma_2} \right)^{1/2}. \tag{1.2}$$

Figure 1.1 shows a new microwave resonator from the University of British Columbia. By measuring the resonant frequency and quality factor of the cavity with sample in and sample out, information can be obtained about the penetration depth λ and surface resistance R_s:

$$\lambda(T) - \lambda(T_0) \propto \Delta f - \Delta f_0, \tag{1.3}$$

$$R_s \propto \left[\frac{1}{Q} - \frac{1}{Q_0} \right], \tag{1.4}$$

where $\Delta f = f(T) - f(T_0)$, f and f_0 are the resonant frequencies, and Q and Q_0 are the quality factors with sample in and sample out respectively.

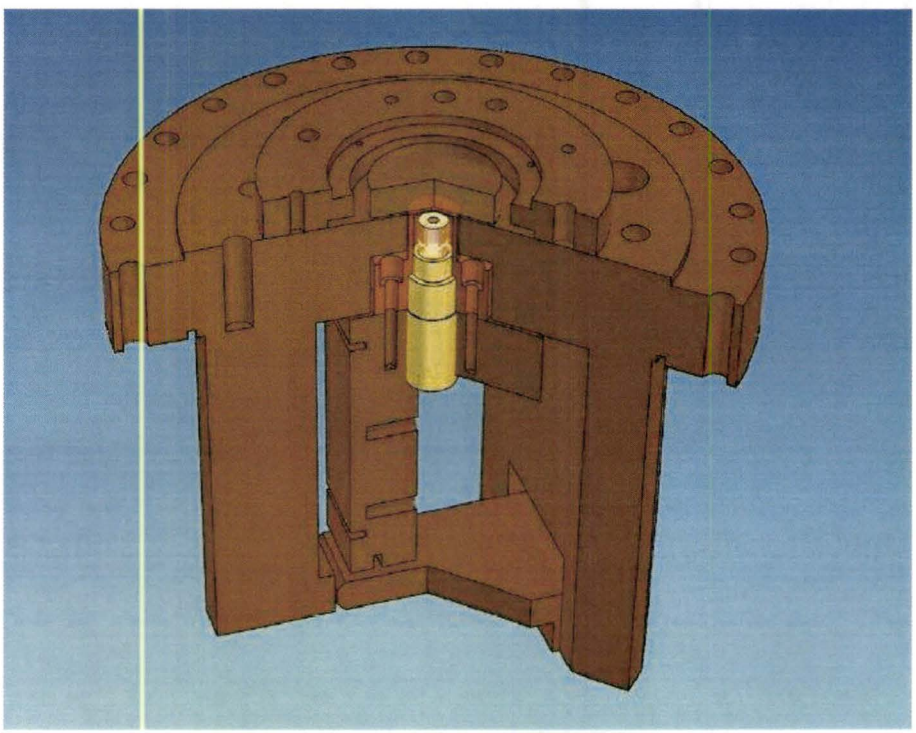

Figure 1.1: The new microwave resonator, Univ. of British Columbia

Penetration depth measurements [8] suggest that $1/\lambda^3 \propto T - T_c$ over a temperature range 5-10 Kelvin wide below T_c, which agrees with the prediction of the 3dXY model. Recently W. N. Hardy *et al* observed the fluctuation peak of the AC conductivity near T_c in high-quality bulk crystals [9], which has previousy been observed mainly in thin films [10, 11].

1.3 Critical Phenomena and Disorder

1.3.1 Universality Class and Critical Exponents

Among all the second order transitions in various systems such as fluids, superfluids, antiferromagnets and superconductors there are some common features. Near the transition power laws of many physical quantities occur, which can be described by a set of critical exponents $\alpha, \beta, \gamma, \nu, \eta$. These indices are independent of the particular properties of the system, and all the phase transitions can be divided into a small number of universality classes determined by the symmetry of the ordered state and the dimensionality of the system.

Another key idea of second order phase transition is scaling, which means that the physical quantities are related to each other by power-laws. Near a second-order phase transition the correlation length ξ has singular dependence on $T - T_c$, dominating all other microscopic lengths near T_c. This leads to the scaling laws which are inequalities or equalities of the critical exponents.

According to the modern theory of critical phenomena, the static universality class for the zero-field normal-superconducting phase transition of a three-dimensional superconductor is 3dXY (three dimensional, complex order parameter). However, the nature of the critical dynamics, which determine the dynamic transport properties, is not as well known. Fisher, Fisher and Huse [12] pointed out that in the critical region $n_s \sim \xi^{2-d}$ and $\tau \sim \xi^z$, therefore from (1.1), the dynamic conductivity scales as

$$\sigma(\omega) \approx \xi^{z+2-d} S_{\pm}(\omega \xi^z), \tag{1.5}$$

where ξ is the correlation length, z is the dynamic critical exponent, and d is the spatial dimensionality. In the limit $T \rightarrow T_c$, the conductivity remains finite, therefore the scaling functions approaches $S_+(x) \approx S_-(x) \approx cx^{[(d-2)/z-1]}$ for $x \rightarrow \infty$. Wickham and Dorsey [1] verified the FFH scaling hypothesis [12] for linear ac conductivity, and showed that the 3d-XY universal scaling function deviates only slightly from its Gaussian form (Fig 1.2). Peligrad and Mehring [2] then took the short-wavelength cutoff into consideration. They calculated the ac fluctuation conductivity in 3D isotropic, 3D anisotrophic and 2D superconductors. Their results showed that the short-wavelength cutoff leads to a breakdown of the scaling property in frequency and temperature.

1.3.2 Disorder

In real systems there are always impurities, defects, dislocations, etc. Will disorder affect the behavior of the system near critical points? A thorough investigation of this problem requires a quantitative renormalization group analysis. Generally, the

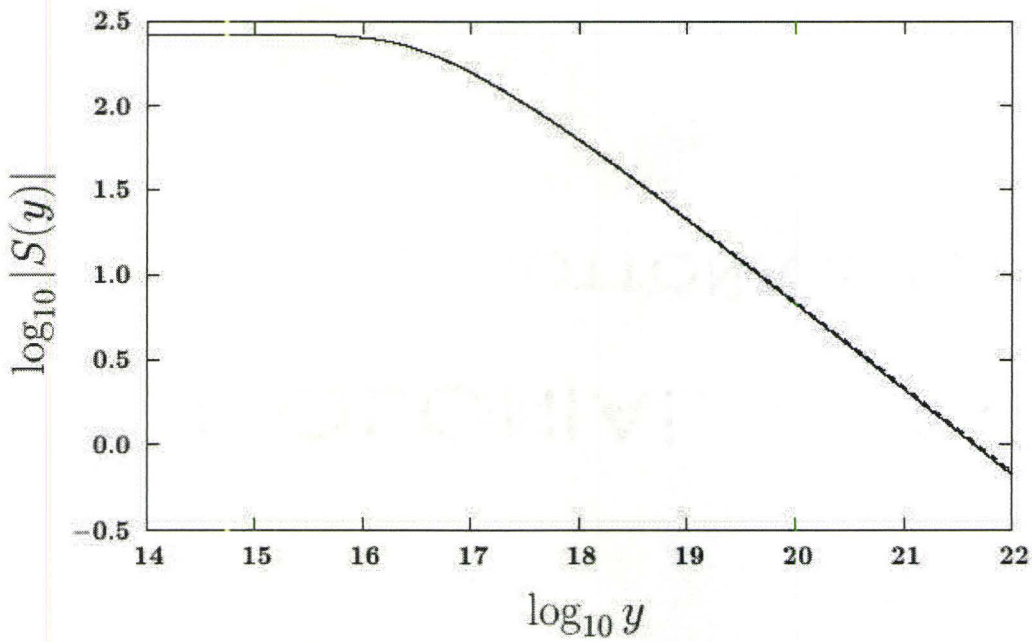

Figure 1.2: The AC conductivity scaling function S(y), for 3dXY critical theory (solid curve) and Gaussian theory (dashed curve) [1].

phase transition remains sharp in the presence of disorder. Whether the behavior of the disordered system differs from the pure system or not is controlled by the Harris criterion [13] $\nu \geq 2/d$, where ν is the correlation length critical exponent and d is spatial dimensionality. If the Harris criterion is satified, the critical exponents will be the same as the clean system. If the Harris criterion is violated, two classes of phenomena will happen [14]: If inhomogeneities remain finite at all length scales, the critical point still displays conventional power-law scaling with a new set of critical exponents. If inhomogeneities increase with coarse graining, the power-law scaling is replaced by exponential scaling.

The study of the fluctuation conductivity in the following chapters was motivated by the inconsistency between theory and experiment. Experimentally it is found that the measured conductivity curves are highly sample-dependent. Therefore we think disorder may play an important role in the critical regimes, and that a distribution of T_c's inside the sample leads to a loss of universality. We use a "lattice model" to study the effects of disorder. The superconductor is treated as a set of lattice sites with a different T_c at different sites. The Ginzburg-Landau hamiltonian and the current operator are written in a discretized formalism, and the conductivity is calculated from the resulting correlation functions, averaged over many disorder configurations.

Chapter 2 presents a calculation of the conductivity of a uniform superconductor for this lattice model. We compare our results for a three-dimensional superconductor with other theoretical investigations. In Chapter 3, disorder effects are taken into

account in our model, and numerical results for a two-dimensional superconductor is presented. Conclusions and plans for future work are in Chapter 4.

Chapter 2

Fluctuation Conductivity in the Gaussian Approximation

2.1 The Lattice Model

2.1.1 Formalism for the Continuum Case

Before I describe the lattice model, I will introduce the calculation for the continous superconductor. A more detailed description can be found in [1].

The free energy of the Ginzburg-Landau model is described by:

$$F = \int d^d r \left(|\nabla \psi|^2 + r_0 |\psi|^2 + b|\psi|^4 + \cdots \right), \tag{2.1}$$

where $r_0 \propto T - T_{c0}$ changes sign at the mean-field transition temperature T_{c0}. At the Gaussian level, the terms higher than second order are negelected for $T > T_c(b = 0)$.

We choose units $\hbar = k_B T_c = 1$ and $m = 1/2$, where m is the mass of a Cooper pair.

In the simplest relaxation model, it is natural to assume that the relaxation rate is proportional to the deviation from equibrium,

$$\frac{\partial \psi}{\partial t} = -\Gamma_0 \frac{\delta F}{\delta \psi^*} + \zeta. \tag{2.2}$$

The noise ζ is assumed to be a Gaussian random function, which has zero mean and is uncorrelated in space and time,

$$\langle \zeta(\mathbf{r}, t) \rangle = 0, \quad \langle \zeta(\mathbf{r}, t) \zeta^*(\mathbf{r}', t') \rangle = 2\Gamma_0 \delta(\mathbf{r} - \mathbf{r}') \delta(t - t'), \tag{2.3}$$

where the factor $2\Gamma_0$ follows from the fluctuation-dissipation theorem [15]. The Fourier transform of the order parameter is defined as:

$$\psi(\mathbf{r}, t) = \int^{\Lambda} \frac{d^d k}{(2\pi)^d} \int \frac{d\omega}{(2\pi)} \psi(\mathbf{k}, \omega) e^{i\mathbf{k}\cdot\mathbf{r} - i\omega t}, \tag{2.4}$$

$$\psi(\mathbf{k}, \omega) = \int d^d r \int dt \psi(\mathbf{r}, t) e^{-(i\mathbf{k}\cdot\mathbf{r} - i\omega t)}, \tag{2.5}$$

where Λ is an ultraviolet cutoff in Ginzburg-Landau theory.

In linear response theory, the response functions are related to the current-current correlation functions at zero external field. The real part of the conductivity can be evaluated by the Kubo formula:

$$\sigma'(\omega) = \frac{1}{2d} \langle \mathbf{J}_s(\omega) \cdot \mathbf{J}_s(-\omega) \rangle |_{E=0}, \tag{2.6}$$

where $\mathbf{J}_s(\omega)$ is $\mathbf{J}_s(\mathbf{k}, \omega)$ at $\mathbf{k} = 0$.

The supercurrent, J_s, is

$$\mathbf{J}_s(\mathbf{r},t) = -ie_0(\psi^*\nabla\psi - \psi\nabla\psi^*), \tag{2.7}$$

where e_0 is the charge of a Cooper pair.

From the above equations we can calculate the conductivity in the Gaussian approximation. A Fourier transform of the TDGL (time-dependent Ginzburg-Landau) equation (2.2) yields:

$$\psi(\mathbf{k},\omega) = \frac{\zeta(\mathbf{k},\omega)}{\Gamma_0(r_0+k^2) - i\omega}. \tag{2.8}$$

Therefore we can calculate the correlation functions:

$$\delta(\mathbf{k}-\mathbf{k}')\delta(\omega-\omega')C(\mathbf{k},\omega) \equiv \langle\psi(\mathbf{k},\omega)\psi^*(\mathbf{k}',\omega')\rangle, \tag{2.9}$$

where

$$\langle\psi(\mathbf{k},\omega)\psi^*(\mathbf{k}',\omega')\rangle = \frac{\langle\zeta(\mathbf{k},\omega)\zeta^*(\mathbf{k}',\omega')\rangle}{\Gamma_0^2(r_0+k^2)^2+\omega^2}, \tag{2.10}$$

We obtain

$$C(\mathbf{k},\omega) = \frac{2\Gamma_0}{\Gamma_0^2(r_0+k^2)^2+\omega^2}. \tag{2.11}$$

From equation (2.6) and (2.7), the real part of the conductivity is:

$$\sigma'(\omega) = \frac{2e_0^2}{d}\int^{\Lambda}\frac{d^dk_1}{(2\pi)^d}\int\frac{d\omega_1}{(2\pi)}k_1^2C(\mathbf{k_1},\omega_1)C(\mathbf{k_1},\omega_1+\omega). \tag{2.12}$$

Using a contour integration for the frequency integral, we get:

$$\sigma'(\omega) = \frac{2e_0^2}{d}\int^{\Lambda}\frac{d^dk_1}{(2\pi)^d}k_1^2\frac{4\Gamma_0^2}{\Gamma_0(r_0+k_1^2)[\omega^2+4\Gamma_0^2(r_0+k_1^2)^2]}. \tag{2.13}$$

Taking the cutoff Λ to be infinity, after another contour integral over k, we get the following form for the conductivity:

$$\sigma'(\omega) = \frac{e_0^2}{2\Gamma_0}\overline{\sigma}\frac{\xi_0^{4-d}}{4-d}S'_G(y_0), \tag{2.14}$$

where y_0 is the scaled frequency:

$$y_0 = \frac{\omega\xi_0^2}{2\Gamma_0}, \tag{2.15}$$

and ξ_0 is the Gaussian order-parameter correlation length:

$$\xi_0 \equiv r_0^{-1/2}, \tag{2.16}$$

and $\overline{\sigma}$ is:

$$\overline{\sigma} = \frac{S_d}{(2\pi)^d}\Gamma(d/2)\Gamma(3-d/2), \tag{2.17}$$

where S_d is the surface area of a d-dimensional unit sphere:

$$S_d = 2\pi^{d/2}\Gamma(d/2). \tag{2.18}$$

The scaling function, $S'_G(y_0)$, is:

$$S'_G(y_0) = \frac{8}{d(d-2)}\frac{1}{y_0^2}\left[1-(1+y_0^2)^{d/4}\cos\left(\frac{d}{2}\arctan y_0\right)\right]. \tag{2.19}$$

Using the Kramers-Kronig relation,

$$\sigma''(\omega) = -P\int\frac{d\omega'}{\pi}\frac{\sigma'(\omega')}{\omega'-\omega}, \tag{2.20}$$

we get the complete form of the scaling function:

$$S_G(y_0) = \frac{8}{d(d-2)}\frac{1}{y_0^2}\left[1-\frac{d}{2}iy_0-(1-iy_0)^{d/2}\right]. \tag{2.21}$$

2.1.2 The Discretized Model

Now we view the superconductor as a number of "lattice sites" with the order parameter $\psi_{\mathbf{R}}$ defined at each site $\mathbf{R}$. Assume a square lattice with nearest spacing l. The Ginzburg-Landau free energy then becomes a summation over lattice sites instead of an integral over $\mathbf{r}$:

$$F = \frac{1}{l^2}\sum_{\mathbf{R},\delta}|\psi_{\mathbf{R}} - \psi_{\mathbf{R}+\delta}|^2 + \sum_{\mathbf{R}} t_0|\psi_{\mathbf{R}}|^2, \tag{2.22}$$

where the ∇^2 in the continuous model is replaced by a summation over the difference between nearest neighbors δ.

The Fourier transformation of the order parameter is:

$$\psi_{\mathbf{R}}(t) = \frac{1}{V}\int \frac{d\omega}{(2\pi)}\sum_{\mathbf{k}} \psi(\mathbf{k},\omega)e^{i\mathbf{k}\cdot\mathbf{R}-i\omega t}, \tag{2.23}$$

$$\psi(\mathbf{k},\omega) = v_0 \int dt \sum_{\mathbf{R}} \psi_{\mathbf{R}}(t)e^{-(i\mathbf{k}\cdot\mathbf{R}-i\omega t)}, \tag{2.24}$$

where $v_0 = l^d$ is the volume of a "unit cell", and $V = Nv_0$ is the total volume of the superconductor.

The correponding form of the TDGL equation is:

$$\frac{\partial\psi_{\mathbf{R}}}{\partial t} = -\Gamma_0\frac{\delta F}{\delta\psi^*_{\mathbf{R}}} + \zeta_{\mathbf{R}}(t), \tag{2.25}$$

and

$$\langle\zeta_{\mathbf{R}}(t)\zeta^*_{\mathbf{R}'}(t')\rangle = 2\Gamma_0\delta_{\mathbf{R},\mathbf{R}'}\delta(t-t'). \tag{2.26}$$

Substituting (2.22) into (2.25), we can solve for $\psi(\mathbf{k},\omega)$

$$\psi(\mathbf{k},\omega)=\frac{\zeta(\mathbf{k},\omega)}{\Gamma_0\left[\frac{1}{l^2}\sum_\delta\left(1-e^{i\mathbf{k}\cdot\delta}\right)+t_0\right]-i\omega}, \tag{2.27}$$

and the correlation functions

$$\langle\psi(\mathbf{k},\omega)\psi^*(\mathbf{k}',\omega')\rangle=\frac{2\Gamma_0 v_0^2[2\pi\delta(\omega-\omega')](N\delta_{\mathbf{k},\mathbf{k}'})}{\Gamma_0^2\left[\frac{1}{l^2}\sum_\delta\left(1-e^{i\mathbf{k}\cdot\delta}\right)+t_0\right]^2+\omega^2}. \tag{2.28}$$

The current operator can also be discretized. For a three-dimensional system,

$$[\mathbf{J}_s(\mathbf{R},t)]_x=-\frac{ie_0}{lv_0}(\psi^*_{\mathbf{R}}\psi_{\mathbf{R}+l\hat{\mathbf{x}}}-\psi_{\mathbf{R}}\psi^*_{\mathbf{R}+l\hat{\mathbf{x}}}), \tag{2.29}$$

$$[\mathbf{J}_s(\mathbf{R},t)]_y=-\frac{ie_0}{lv_0}(\psi^*_{\mathbf{R}}\psi_{\mathbf{R}+l\hat{\mathbf{y}}}-\psi_{\mathbf{R}}\psi^*_{\mathbf{R}+l\hat{\mathbf{y}}}), \tag{2.30}$$

$$[\mathbf{J}_s(\mathbf{R},t)]_z=-\frac{ie_0}{lv_0}(\psi^*_{\mathbf{R}}\psi_{\mathbf{R}+l\hat{\mathbf{z}}}-\psi_{\mathbf{R}}\psi^*_{\mathbf{R}+l\hat{\mathbf{z}}}). \tag{2.31}$$

After Fourier transformation,

$$[\mathbf{J}_s(\omega)]_x=[\mathbf{J}_s(\mathbf{k},\omega)]_x|_{\mathbf{k}=0}=\frac{2e_0}{lv_0}\frac{1}{V}\int\frac{d\omega_1}{2\pi}\sum_{\mathbf{k_1}}(\sin k_{1x}l)\psi^*(\mathbf{k_1},\omega_1)\psi(\mathbf{k_1},\omega_1+\omega), \tag{2.32}$$

$$[\mathbf{J}_s(\omega)]_y=\frac{2e_0}{lv_0}\frac{1}{V}\int\frac{d\omega_1}{2\pi}\sum_{\mathbf{k_1}}(\sin k_{1y}l)\psi^*(\mathbf{k_1},\omega_1)\psi(\mathbf{k_1},\omega_1+\omega), \tag{2.33}$$

$$[\mathbf{J}_s(\omega)]_z=\frac{2e_0}{lv_0}\frac{1}{V}\int\frac{d\omega_1}{2\pi}\sum_{\mathbf{k_1}}(\sin k_{1z}l)\psi^*(\mathbf{k_1},\omega_1)\psi(\mathbf{k_1},\omega_1+\omega). \tag{2.34}$$

Using the Kubo formula

$$\sigma'(\omega) = \frac{1}{2d}\frac{1}{V}\langle \mathbf{J}_s(\omega)\cdot\mathbf{J}_s(-\omega)\rangle|_{E=0}, \tag{2.35}$$

the real part of the conductivity is given as:

$$\sigma'_{3d}(\omega) = \frac{2e_0^2}{d}\frac{1}{V^2}\frac{1}{v_0^2}\frac{1}{l^2}\int\frac{d\omega_1}{2\pi}\int\frac{d\omega_2}{2\pi}\sum_{\mathbf{k_1}}\sum_{\mathbf{k_2}}(\sin k_{1x}l\sin k_{2x}l + \sin k_{1y}l\sin k_{2y}l$$
$$+\sin k_{1z}l\sin k_{2z}l)\langle\psi^*(\mathbf{k_1},\omega_1)\psi(\mathbf{k_2},\omega_2-\omega)\rangle\langle\psi(\mathbf{k_1},\omega_1+\omega)\psi^*(\mathbf{k_2},\omega_2)\rangle. \tag{2.36}$$

Substituting (2.28) into (2.36) and integrating over the frequency, we get the conductivity in the following form:

$$\sigma'_{3d}(\omega) = \frac{2e_0^2}{d}(4\Gamma_0)\frac{1}{V}\frac{1}{l^2}\sum_{\mathbf{k_1}}\frac{(\sin^2 k_{1x}l+\sin^2 k_{1y}l+\sin^2 k_{1z}l)}{\frac{1}{l^2}[6-2(\cos k_{1x}l+\cos k_{1y}l+\cos k_{1z}l)]+t_0}$$
$$\times\frac{1}{\omega^2+4\Gamma_0^2\left\{\frac{1}{l^2}[6-2(\cos k_{1x}l+\cos k_{1y}l+\cos k_{1z}l)]+t_0\right\}^2} \tag{2.37}$$

To compare with equation (2.14), the conductivity can be written as:

$$\sigma'_{3d}(\omega) = \frac{e_0^2}{2\Gamma_0}\frac{\xi_0}{8\pi}S'(t,\nu), \tag{2.38}$$

where $\xi_0 = t_0^{-1/2}$ and

$$S'(t,\nu) = \frac{4}{3\pi^2 t^{3/2}}\frac{(2\pi)^3}{N}\sum_{x,y,z}^{-\frac{N-1}{N}\pi,\ldots,\pi}\frac{\sin^2 x+\sin^2 y+\sin^2 z}{[6-2(\cos x+\cos y+\cos z)+t]}$$
$$\times\frac{1}{\nu^2+\left\{\frac{1}{t}[6-2(\cos x+\cos y+\cos z)]+1\right\}^2}, \tag{2.39}$$

where $x = k_{1x}l$, $y = k_{1y}l$, $z = k_{1z}l$ and the scaled temperature t and frequency ν is defined as:

$$t \equiv t_0 l^2, \tag{2.40}$$

$$\nu \equiv \frac{\omega}{2\Gamma_0 t_0}. \tag{2.41}$$

In the limit $N = V/v_0 \to \infty$, $\sum_{\mathbf{k_1}} \to V \int \frac{d\mathbf{k_1}}{(2\pi)^3}$, and

$$S'(t,\nu) = \frac{4}{\pi^2 t^{3/2}} \int_{-\pi}^{\pi} dx \int_{-\pi}^{\pi} dy \int_{-\pi}^{\pi} dz \frac{\sin^2 x + \sin^2 y + \sin^2 z}{[6 - 2(\cos x + \cos y + \cos z) + t]} \times \frac{1}{\nu^2 + \left\{\frac{1}{t}[6 - 2(\cos x + \cos y + \cos z)] + 1\right\}^2}, \tag{2.42}$$

Similarly, for the two dimensional system, we have:

$$\sigma'_{2d}(\omega) = \frac{e_0^2}{\Gamma_0} \frac{\xi_0^2}{8\pi} S'(t,\nu), \tag{2.43}$$

where

$$S'(t,\nu) = \frac{2}{\pi t} \frac{(2\pi)^2}{N} \sum_{x,y}^{-\frac{N-1}{N}\pi,\ldots,\pi} \frac{\sin^2 x + \sin^2 y}{[4 - 2(\cos x + \cos y) + t]} \times \frac{1}{\nu^2 + \left\{\frac{1}{t}[4 - 2(\cos x + \cos y)] + 1\right\}^2}. \tag{2.44}$$

In the large N limit,

$$S'(t,\nu) = \frac{2}{\pi t} \int_{-\pi}^{\pi} dx \int_{-\pi}^{\pi} dy \frac{\sin^2 x + \sin^2 y}{[4 - 2(\cos x + \cos y) + t]} \times \frac{1}{\nu^2 + \left\{\frac{1}{t}[4 - 2(\cos x + \cos y)] + 1\right\}^2}. \tag{2.45}$$

It can be easily verified that in the $l \to 0$ limit, equation (2.42) and (2.45) approach the result of the continuous model (2.19).

2.1.3 Dimensional Analysis

It is worthy to point out the dimensions of the Ginzburg-Landau free energy, the correlation functions and the conductivity. The G-L free energy in equation (2.1) is

dimensionless, so

$$\left[\int d^d r|\nabla\psi|^2\right] = 1 \Longrightarrow L^d \cdot L^{-2}[\psi]^2 = 1, \tag{2.46}$$

where we use $[\ldots]$ to denote the dimensions of the quantity enclosed.

Hence,

$$[\psi(\mathbf{r},t)] = L^{1-d/2}, \tag{2.47}$$

where L is the unit of length.

Then $[r_0]$ can be determined.

$$\left[\int d^d r r_0|\psi(\mathbf{r},t)|^2\right] = 1 \Longrightarrow [r_0] = L^{-2}, \tag{2.48}$$

which agrees with our previous definition $\xi_0 = r_0^{-1/2}$.

Then we have the units of the parameters in the TDGL equation (2.2),

$$\begin{aligned}[\zeta(\mathbf{r},t)] &= L^{1-d/2}\cdot T^{-1},\\ [\Gamma_0] &= L^2\cdot T^{-1},\end{aligned} \tag{2.49}$$

where T is the unit of time.

And there follows

$$[\langle\psi(\mathbf{r},t)\psi(\mathbf{r}',t')\rangle] = [\psi]^2 = L^{2-d}. \tag{2.50}$$

In k space,

$$[\psi(\mathbf{k},\omega)] = [\psi(\mathbf{r},t)]\cdot L^d \cdot T = L^{1+d/2}\cdot T, \tag{2.51}$$

$$[\langle\psi(\mathbf{k},\omega)\psi(\mathbf{k}',\omega')\rangle] = L^{2+d}\cdot T^2, \tag{2.52}$$

$$[C(\mathbf{k},\omega)] = L^2 \cdot T \tag{2.53}$$

From equation (2.12),

$$[\sigma(\omega)] = [C(\mathbf{k},\omega)]^2 \cdot L^{-2-d} \cdot T^{-1} \cdot C^2 = C^2 \cdot L^{2-d} \cdot T, \tag{2.54}$$

where C denotes the unit of charge.

For the discretized model, an additional parameter l with dimension L is introduced. $\psi(\mathbf{R})$ has dimension L and $[t_0] = [r_0] = L^{-2}$. Since the analysis is much similar to the continuous case, we will not go through the details here. I will end this part by pointing out that from (2.38) and (2.43), it can be seen that the results of the lattice model has the same dimension as the continuous model. Therefore the dimensional analysis provides a tool to test the validity of the models before we calculate the conductivity numerically.

Notice that at the beginning, we take $\hbar = k_B T_c = 1$ and $m = 1/2$ for convenience. To connect our result to real systems, we have to take these constants into account.

2.2 Numerical Results and Discussion

2.2.1 Scaling Functions

We carry out the integration numerically by Mathematica for the two-dimensional and three-dimensional systems and plot our scaling functions $S'(t,\nu)$ versus the scaled

frequency ν at different values of t in comparison with the scaling functions for the continous system. The two-dimensional case and three-dimensional case are plotted in fig. 2.1 and fig. 2.2, respectively.

The "lattice sites" in our model is by no means the crystal lattice; The "lattice constant" l, is not a microscopic quantity. It is related to the coarse graining of the Ginzburg-Landau theory. When we discretize the superconductor, the order parameter is uniform inside a "unit cell" with volume $v_0 = l^d$. This is equivalent to introducing a short-wavelength cutoff $\Lambda \propto 1/l$ to the Ginzburg-Landau theory.

The scaling function $S'(y_0)$ break into a set of curves for different values of t. At fixed t, the scaling functions is similar to $S'(y_0)$ and approaches a finite value at $\nu = 0$. This implies that if we keep the "lattice constant" l proportional to the correlation length $\xi_0 = \xi_0(T)$, the scaling property is preserved. In general, the fluctuation conductivity for the lattice model is lowered with respect to the continuous model. Dimensionality plays an important role in our problem: In three-dimensional systems the decrease is more remarkable than two-dimensional case. At small values of t and ν, the scaling functions $S'(t, \nu)$ approaches $S'(y_0)$.

2.2.2 Comparison with Other Theoretical Work

There has been theoretical work investigating with the short-wavelength cutoff effects on AC fluctuation conductivity by Peligrad and Mehring [2]. They calculated the conductivity with a finite cutoff for the three-dimensional isotropic and anisotropic

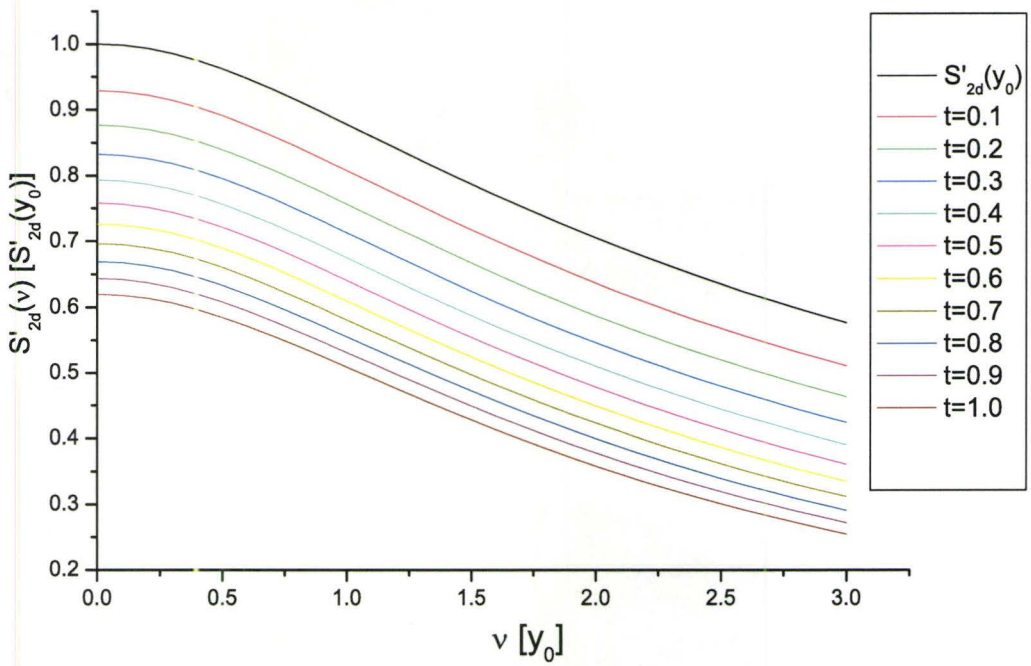

Figure 2.1: The 2d AC conductivity scaling function $S'(t,\nu)$ vs. ν plotted at $t = 0.1, 0.2, \ldots, 1$,compared with the scaling function $S'(y_0)$ for the contious case.

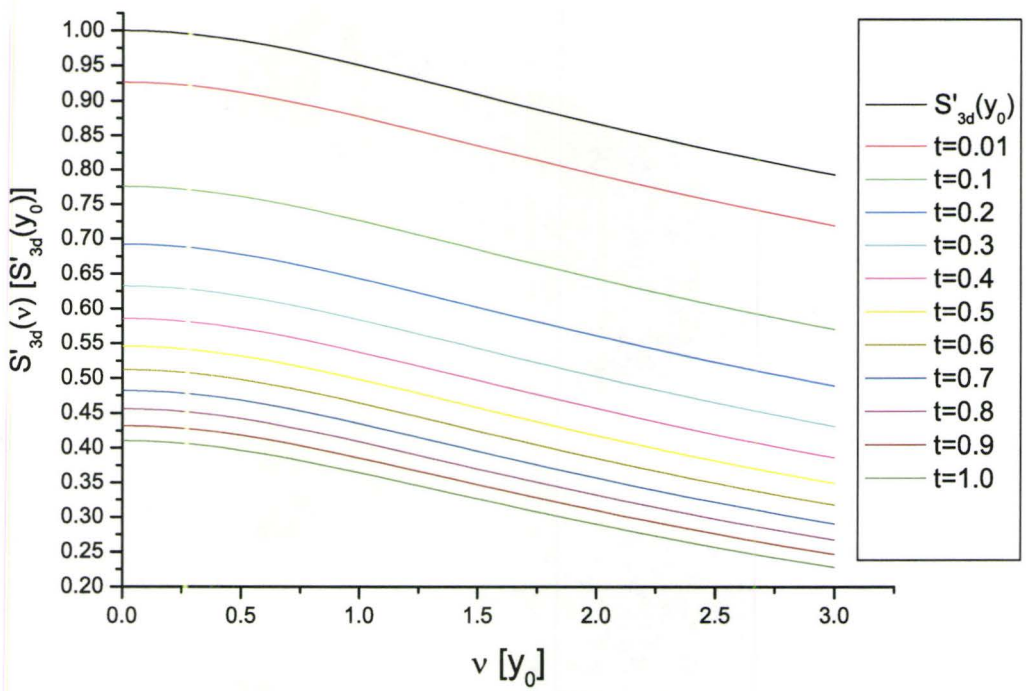

Figure 2.2: The 3d AC conductivity scaling function $S'(t, \nu)$ vs. ν plotted at $t = 0.01, 0.1, 0.2, \ldots, 1$,compared with the scaling function $S'(y_0)$ for the contious case.

cases as well as two-dimensional thin films. They introduce a dimensionless parameter Λ and set the cutoff in k_x to be $\Lambda/\xi_0(T=0)$, where $\xi_0(T=0)$ is the correlation length at zero temperature. In the three-dimensional isotropic case, the same cutoff applies to k_y and k_z, and the integral in k space has an upper limit $k_{max} = \sqrt{3}/\Lambda$. The real part of the AC fluctuation conductivity is obtained in the following form

$$\sigma_1(\omega, T, \Lambda) = \frac{e^2}{32\hbar\xi_0(T=0)} \left(\frac{\xi(T)}{\xi_0(T=0)} \right)^{z-1} S_1(\omega, T, \Lambda), \tag{2.55}$$

where

$$S_1(\omega, T, \Lambda) = \frac{1}{3\pi\Omega^2}[P_-(P_+^2+2)L + 2P_+(P_-^2-2)A + 16\arctan(Q)], \tag{2.56}$$

$$P_\pm = \sqrt{2}\sqrt{\sqrt{\Omega^2+1}\pm 1}, \tag{2.57}$$

$$L = \ln\left(\frac{2+Q^2+(Q-P_-)^2}{2+Q^2+(Q+P_-)^2}\right), \tag{2.58}$$

$$A = \arctan\left(\frac{2Q+P_-}{P_+}\right) + \arctan\left(\frac{2Q-P_-}{P_+}\right), \tag{2.59}$$

and the dimensionless variable

$$\Omega(\omega, T) = \frac{\pi}{16}\frac{\hbar\omega}{k_B T_c}\left(\frac{\xi(T)}{\xi_0(T=0)}\right)^z. \tag{2.60}$$

Figure 2.3 shows a set of S_1 curves ploted at three different frequencies. The cutoff parameter Λ is 0.5. The dashed curve shows the S_1 curve at $\Lambda = \infty$, which is only a function of the scaled frequency Ω.

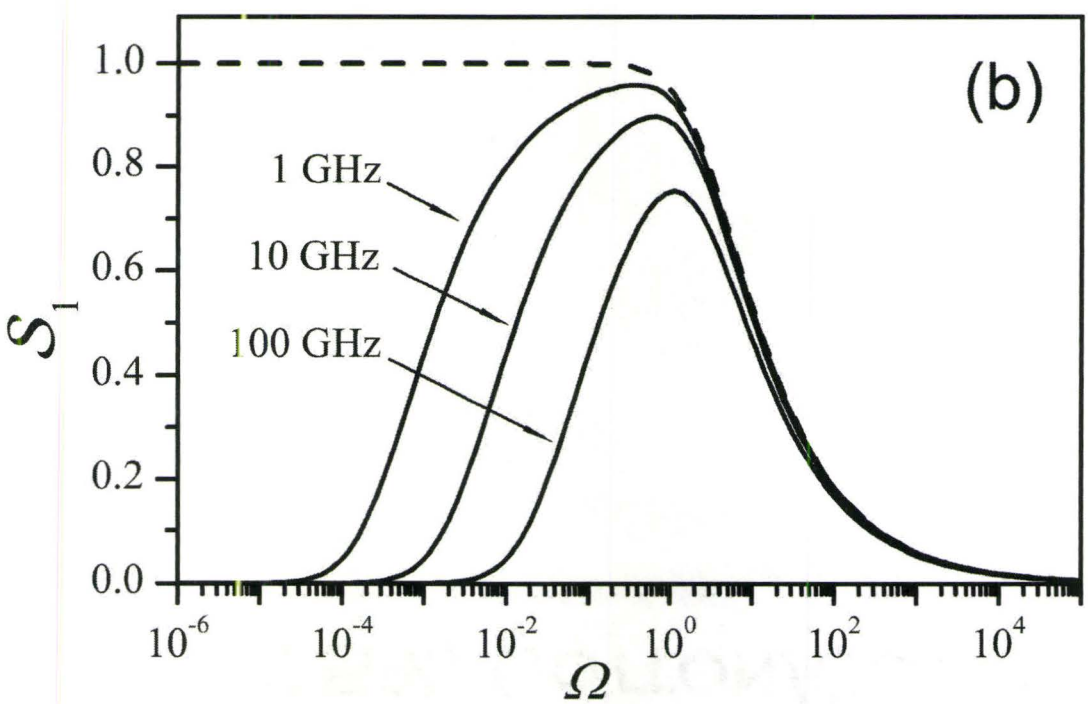

Figure 2.3: S_1 curves plotted at $\omega/2\pi = 1, 10, 100$GHz [2].

To compare our result with the above theoretical investigations [2], we plot our S' curves at fixed frequencies and fixed l, which corresponds to a fixed cutoff Λ. l can be approximately determined by

$$k_x^{max} = \Lambda/\xi_0(T=0) = \pi/l \Longrightarrow l = \pi\xi_0(T=0)/\Lambda = 2\pi\xi_0(T=0). \tag{2.61}$$

We choose T_c to be the value in [2], 84.04K. For every ν (which is Ω in the above equations), we can find the value of t and then calculate $S'(t,\nu)$ numerically. Our result is plotted in Fig. 2.4.

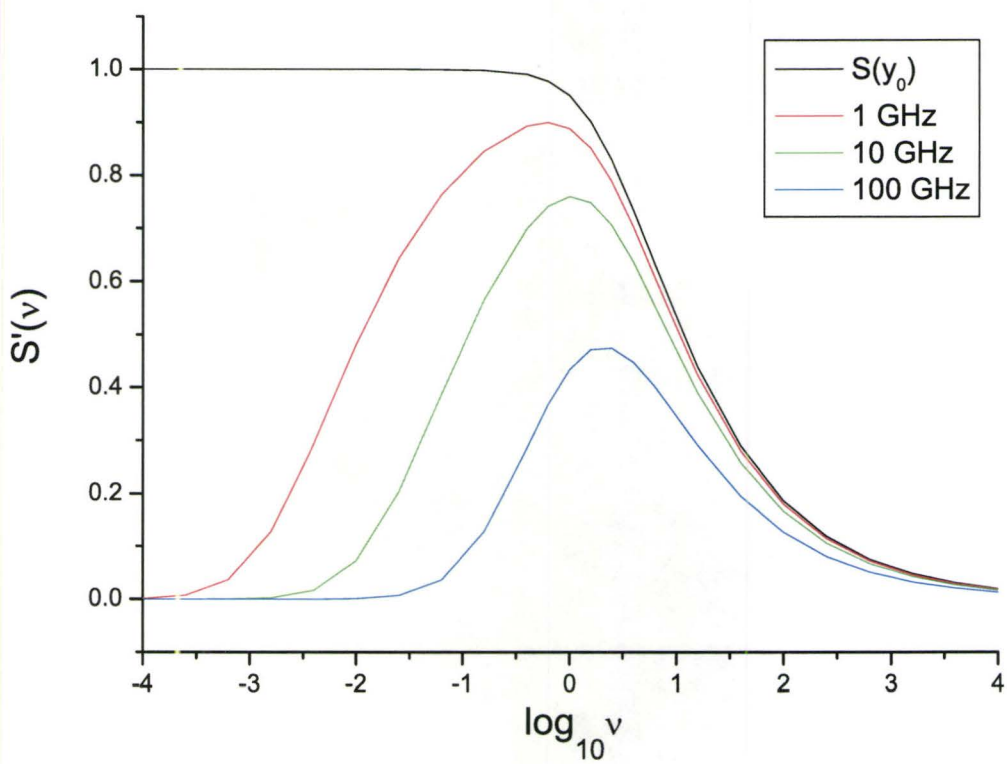

Figure 2.4: The 3d AC conductivity scaling function $S'(t,\nu)$ vs. ν plotted at three diffenent frequencies compared with $S'(y_0)$

It can be seen from Fig. 2.3 and Fig. 2.4 our scaling functions agrees well qualitively with [2]. Note that in equation (2.56), there are three parameters, Λ, T, and ω. In figure 2.3, $\Lambda \propto \xi_0(T = 0)$ is a constant, and the scaling functions S_1 approaches zero at small Ω. In our model there are only two parameters, which is the ratio of the "lattice constant" l to the correlation length at T, and the scaled frequency ν. If we keep $l/\xi(T)$ fixed as in fig. 2.1, at small ν the scaling functions approach a finite value instead of zero.

Peligrad and Mehring also discussed the cutoff effects on the imaginary part of the conductivity. The effects are small compared with the real part, and close to T_c the curve with and without the cutoff are indistinguishable. The scaling functions for the 3d anisotropic superconductors and 2d thin films were also discussed. These issues are beyond the scope of this thesis, but we will possibly calculate the imaginary part of the conductivity in our future work.

Chapter 3

Disorder Effects

3.1 Real Space Formalism

Next we consider the effects of disorder in superconductors. Assuming the critical temperature is position-dependent, we replace the parameter t_0 by $t_{\mathbf{R}}$:

$$F = \frac{1}{l^2} \sum_{\mathbf{R},\delta} |\psi_{\mathbf{R}} - \psi_{\mathbf{R}+\delta}|^2 + \sum_{\mathbf{R}} t_{0\mathbf{R}} |\psi_{\mathbf{R}}|^2, \tag{3.1}$$

where $t_{0\mathbf{R}} \propto T - T_c(\mathbf{R})$.

Let

$$t_{\mathbf{R}} = l^2 t_{0\mathbf{R}} = t + \delta t_{\mathbf{R}}, \tag{3.2}$$

where t is the average of $t_{\mathbf{R}}$ and $\delta t_{\mathbf{R}}$ is the deviation.

From the TDGL equation (2.25) we get:

$$\frac{\partial \psi_{\mathbf{R}}(t)}{\partial t} = -\Gamma_0 \left\{ \frac{1}{l^2} \sum_{\delta} [\psi_{\mathbf{R}}(t) - \psi_{\mathbf{R}+\delta}(t)] + t_{0\mathbf{R}} \psi_{\mathbf{R}}(t) \right\} + \zeta_{\mathbf{R}}(t) \tag{3.3}$$

To solve the TDGL equation for the disordered case, we seperate the time and spatial dependence of the order parameter. Assume that the order parameter can be expanded in a complete set of orthogonal functions:

$$\psi_{\mathbf{R}}(t) = \int \frac{d\omega}{2\pi} \sum_j \phi^j_{\mathbf{R}} a^j(\omega) e^{-i\omega t}, \tag{3.4}$$

where $\{\phi^j_{\mathbf{R}}\}$ satisfy:

$$\frac{1}{l^2} \sum_{\delta} (\phi^j_{\mathbf{R}} - \phi^j_{\mathbf{R}+\delta}) + t_{0\mathbf{R}} \phi^j_{\mathbf{R}} = \lambda_j \phi^j_{\mathbf{R}}, \tag{3.5}$$

In a matrix formalism, we write the above equation as:

$$H_0 \begin{pmatrix} \phi^j_1 \\ \vdots \\ \phi^j_N \end{pmatrix} = \lambda_j \begin{pmatrix} \phi^j_1 \\ \vdots \\ \phi^j_N \end{pmatrix} \tag{3.6}$$

H_0 is a $N \times N$ matrix with nearest neighbor hopping and periodic boundary conditions, and the $\{\phi^j_{\mathbf{R}}\}$ are the "eigenvectors" of H_0, which satisfy the orthnormal and complete conditions:

$$\sum_{\mathbf{R}} (\phi^j_{\mathbf{R}})^* \phi^{j'}_{\mathbf{R}} = \delta_{j,j'}, \tag{3.7}$$

$$\sum_{j} (\phi^j_{\mathbf{R}})^* \phi^j_{\mathbf{R}'} = \delta_{\mathbf{R},\mathbf{R}'} \tag{3.8}$$

Substituting (3.4) into (3.3), we obtain the expression for $a^j(\omega)$:

$$a^j(\omega) = \frac{\sum_{\mathbf{R}} (\phi^j_{\mathbf{R}})^* \zeta_{\mathbf{R}}(\omega)}{\Gamma_0 \lambda_j - i\omega}, \tag{3.9}$$

and the correlation functions can be calculated as:

$$\langle \psi_{\mathbf{R}}(\omega)\psi^*_{\mathbf{R}'}(\omega')\rangle = 4\pi\Gamma_0\delta(\omega-\omega')\sum_j \frac{(\phi^j_{\mathbf{R}})^*\phi^j_{\mathbf{R}'}}{(\Gamma_0\lambda_j)^2+\omega^2} \tag{3.10}$$

The conductivity can be written as the correlation of the current operator in real space as:

$$\sigma'(\omega) = \frac{1}{2d}\frac{1}{V}v_0^2\sum_{\mathbf{R}}\sum_{\mathbf{R}'}\langle \mathbf{J}_s(\mathbf{R},\omega)\cdot\mathbf{J}_s(\mathbf{R}',-\omega)\rangle \tag{3.11}$$

Now consider the current operator in real space. Take the $\hat{x}$ component,

$$\begin{aligned}[\mathbf{J}_s(\mathbf{R},\omega)]_x &= \int dt e^{i\omega t}\,[\mathbf{J}_s(\mathbf{R},t)]_x \\ &= -\frac{ie_0}{lv_0}\int\frac{d\omega_1}{2\pi}\left[\psi^*_{\mathbf{R}}(\omega_1)\psi_{\mathbf{R}+l\hat{\mathbf{x}}}(\omega_1+\omega)-\psi^*_{\mathbf{R}+l\hat{\mathbf{x}}}(\omega_1)\psi_{\mathbf{R}}(\omega_1+\omega)\right]\end{aligned} \tag{3.12}$$

Assume the lattice has N sites. Define a $N\times N$ matrix operator $\mathbf{T}(\mathbf{R})$ which satisfies:

$$\begin{aligned}&\psi^*_{\mathbf{R}}(\omega_1)\psi_{\mathbf{R}+l\hat{\mathbf{x}}}(\omega_1+\omega)-\psi^*_{\mathbf{R}+l\hat{\mathbf{x}}}(\omega_1)\psi_{\mathbf{R}}(\omega_1+\omega) \\ &= \begin{pmatrix}\psi^*_1(\omega_1) & \dots & \psi^*_{\mathbf{R}}(\omega_1) & \dots & \psi^*_N(\omega_1)\end{pmatrix}[\mathbf{T}(\mathbf{R})]_x\begin{pmatrix}\psi_1(\omega_1+\omega)\\ \vdots \\ \psi_{\mathbf{R}}(\omega_1+\omega)\\ \vdots \\ \psi_N(\omega_1+\omega)\end{pmatrix} \\ &= \langle\psi(\omega_1)|[\mathbf{T}(\mathbf{R})]_x|\psi(\omega_1+\omega)\rangle,\end{aligned} \tag{3.13}$$

where

$$\psi(\omega) \equiv \begin{pmatrix} \psi_1(\omega) \\ \vdots \\ \psi_{\mathbf{R}}(\omega) \\ \vdots \\ \psi_N(\omega) \end{pmatrix}, \tag{3.14}$$

then the summation over R and R' in equation (3.11) can be carried out as a summation over the matrix $\mathbf{T}(\mathbf{R})$:

$$\sum_{\mathbf{R}} [\mathbf{J}_s(\mathbf{R},\omega)]_x = -\frac{ie_0}{lv_0} \int \frac{d\omega_1}{2\pi} \langle \psi(\omega_1)|\mathbf{T}_x|\psi(\omega_1+\omega)\rangle, \tag{3.15}$$

where $\mathbf{T}_x = \sum_{\mathbf{R}} [\mathbf{T}(\mathbf{R})]_x$.

Therefore the correlation function of the current operator is:

$$\begin{aligned}
\sum_{\mathbf{R}} \sum_{\mathbf{R}'} \langle \mathbf{J}_s(\mathbf{R},\omega) \cdot \mathbf{J}_s(\mathbf{R}',-\omega)\rangle &= \langle \sum_{\mathbf{R}} \mathbf{J}_s(\mathbf{R},\omega) \cdot \sum_{\mathbf{R}'} \mathbf{J}_s(\mathbf{R}',-\omega)\rangle \\
&= -\left(\frac{e_0}{lv_0}\right)^2 \int \frac{d\omega_1}{2\pi} \int \frac{d\omega_2}{2\pi} [\langle\langle \psi(\omega_1)|\mathbf{T}_x|\psi(\omega_1+\omega)\rangle \langle \psi(\omega_2)|\mathbf{T}_x|\psi(\omega_2-\omega)\rangle\rangle \\
&\quad + \langle\langle \psi(\omega_1)|\mathbf{T}_y|\psi(\omega_1+\omega)\rangle \langle \psi(\omega_2)|\mathbf{T}_y|\psi(\omega_2-\omega)\rangle\rangle \\
&\quad + \langle\langle \psi(\omega_1)|\mathbf{T}_z|\psi(\omega_1+\omega)\rangle \langle \psi(\omega_2)|\mathbf{T}_z|\psi(\omega_2-\omega)\rangle\rangle] \\
&= -\left(\frac{e_0}{lv_0}\right)^2 \int \frac{d\omega_1}{2\pi} \int \frac{d\omega_2}{2\pi} \sum_{i,j} \sum_{i',j'} [(\mathbf{T}_x)_{ij}(\mathbf{T}_x)_{i'j'} + (\mathbf{T}_y)_{ij}(\mathbf{T}_y)_{i'j'} \\
&\quad + (\mathbf{T}_z)_{ij}(\mathbf{T}_z)_{i'j'}] \langle \psi_i^*(\omega_1)\psi_j(\omega_2-\omega)\rangle \langle \psi_{i'}^*(\omega_2)\psi_{j'}(\omega_1+\omega)\rangle.
\end{aligned} \tag{3.16}$$

Using (3.10) and (3.16), and after the frequency integral, we have:

$$\begin{aligned}
&\sum_{\mathbf{R}}\sum_{\mathbf{R}'}\langle \mathbf{J}_s(\mathbf{R},\omega)\cdot\mathbf{J}_s(\mathbf{R}',-\omega)\rangle \\
&\quad = -\left(\frac{e_0}{lv_0}\right)^2 2\Gamma_0 \sum_{i,j}\sum_{i',j'}[(\mathbf{T}_x)_{ij}(\mathbf{T}_x)_{i'j'}+(\mathbf{T}_y)_{ij}(\mathbf{T}_y)_{i'j'}+(\mathbf{T}_z)_{ij}(\mathbf{T}_z)_{i'j'}] \\
&\qquad \sum_{k,k'}\frac{\lambda_k+\lambda_{k'}}{\lambda_k\lambda_{k'}[\omega^2+\Gamma_0^2(\lambda_k+\lambda_{k'})^2]}(\phi_i^k)^*\phi_{j'}^k(\phi_{i'}^{k'})^*\phi_j^{k'} \\
&\quad = -\left(\frac{e_0}{lv_0}\right)^2 2\Gamma_0 \sum_{k,k'}\frac{\lambda_k+\lambda_{k'}}{\lambda_k\lambda_{k'}[\omega^2+\Gamma_0^2(\lambda_k+\lambda_{k'})^2]} \\
&\qquad [(\mathbf{K}_x)_{kk'}(\mathbf{K}_x)_{k'k}+(\mathbf{K}_y)_{kk'}(\mathbf{K}_y)_{k'k}+(\mathbf{K}_z)_{kk'}(\mathbf{K}_z)_{k'k}], \qquad (3.17)
\end{aligned}$$

where

$$\begin{aligned}
(\mathbf{K}_x)_{k'k} &= \sum_{i,j}(\phi_i^k)^*(\mathbf{T}_x)_{ij}\phi_j^{k'}, \\
(\mathbf{K}_y)_{k'k} &= \sum_{i,j}(\phi_i^k)^*(\mathbf{T}_y)_{ij}\phi_j^{k'}, \\
(\mathbf{K}_z)_{k'k} &= \sum_{i,j}(\phi_i^k)^*(\mathbf{T}_z)_{ij}\phi_j^{k'}. \qquad (3.18)
\end{aligned}$$

The matrix $\mathbf{K}_x$ can be viewed as the transformation of $\mathbf{T}_x$ from the $\mathbf{R}$ "basis" into the $\{\phi_i^k\}$ "basis":

$$\mathbf{K}_x = U^\dagger \mathbf{T}_x U, \qquad (3.19)$$

where

$$U = \begin{pmatrix} \phi_1^1 & \phi_1^2 & \cdots & \phi_1^N \\ \phi_2^1 & \phi_2^2 & \cdots & \phi_2^N \\ \vdots & \ddots & \ddots & \vdots \\ \phi_N^1 & \cdots & \cdots & \phi_N^N \end{pmatrix} \qquad (3.20)$$

and $U^\dagger = U^{-1}$.

The conductivity is:

$$\sigma'(\omega) = \frac{e_0^2}{d}\frac{l^{4-d}}{\Gamma_0}\frac{1}{N}\sum_{k,k'}\frac{\epsilon_k+\epsilon_{k'}}{\epsilon_k\epsilon_{k'}[4\nu^2t^2+(\epsilon_k+\epsilon_{k'})^2]}$$
$$[(\mathbf{K}_x)_{kk'}(\mathbf{K}_x)_{k'k}+(\mathbf{K}_y)_{kk'}(\mathbf{K}_y)_{k'k}+(\mathbf{K}_z)_{kk'}(\mathbf{K}_z)_{k'k}], \tag{3.21}$$

where ϵ_k, t, ν are dimensionless and

$$\epsilon_k \equiv \lambda_k l^2, \quad t \equiv t_0 l^2, \quad \nu \equiv \frac{\omega}{2\Gamma_0 t_0}. \tag{3.22}$$

Then we have the scaling functions for the three-dimensional case

$$\sigma'_{3d}(\omega) = \frac{e_0^2}{2\Gamma_0}\frac{\xi_0}{8\pi}\mathcal{S}'_{3d}(t,\nu), \tag{3.23}$$

where

$$\mathcal{S}'_{3d}(t,\nu) = \frac{16\pi}{3}t^{1/2}\frac{1}{N}\sum_{k,k'}\frac{\epsilon_k+\epsilon_{k'}}{\epsilon_k\epsilon_{k'}[4\nu^2t^2+(\epsilon_k+\epsilon_{k'})^2]}$$
$$[(\mathbf{K}_x)_{kk'}(\mathbf{K}_x)_{k'k}+(\mathbf{K}_y)_{kk'}(\mathbf{K}_y)_{k'k}+(\mathbf{K}_z)_{kk'}(\mathbf{K}_z)_{k'k}]. \tag{3.24}$$

And for the two-dimensional case, similarly we have:

$$\sigma'_{2d}(\omega) = \frac{e_0^2}{\Gamma_0}\frac{\xi_0^2}{8\pi}\mathcal{S}'_{2d}(t,\nu), \tag{3.25}$$

where

$$\mathcal{S}'_{2d}(t,\nu) = \frac{4\pi t}{N}\sum_{k,k'}\frac{\epsilon_k+\epsilon_{k'}}{\epsilon_k\epsilon_{k'}[4\nu^2t^2+(\epsilon_k+\epsilon_{k'})^2]}[(\mathbf{K}_x)_{kk'}(\mathbf{K}_x)_{k'k}+(\mathbf{K}_y)_{kk'}(\mathbf{K}_y)_{k'k}]. \tag{3.26}$$

If there is no disorder, $t_{\mathbf{R}} = t_0$, equantions (3.24) and (3.26) are equivalent to the corresponding equations (2.39) and (2.44) in Chapter 2.

3.2 Computational Analysis

3.2.1 Methods of Simulation

We calculate the conductivity using Fortran 90 programs. The program is organized into the following steps:

1. Generate a $N \times N$ matrix H with periodic boundary conditions and nearest neighbor hopping. Disorder is represented by adding a random number to the diagonal elements. The operators $\mathbf{T}_x$,$\mathbf{T}_y$ and $\mathbf{T}_z$ are also generated.

2. The matrix is diagonalized using LAPACK (Linear Algebra PACKage) routines, and the eigenvalues ϵ_j and eigenvectors $\{\phi^j_{\mathbf{R}}\}$ is obtained.

3. Transform $\mathbf{T}_x$,$\mathbf{T}_y$ and $\mathbf{T}_z$ to the $\{\phi^j_{\mathbf{R}}\}$ basis to find $\mathbf{K}_x$,$\mathbf{K}_y$ and $\mathbf{K}_z$. This is just matrix multiplication in our program. To make the program efficient, we use a BLAS(Basic Linear Algebra Subprograms) routine to perform the matrix multiplication.

4. Using equation (3.24) and (3.26), the scaling functions are calculated.

We write equation (3.5) as

$$\sum_{\delta}(\phi^j_{\mathbf{R}} - \phi^j_{\mathbf{R}+\delta}) + t_{\mathbf{R}}\phi^j_{\mathbf{R}} = \epsilon_j\phi^j_{\mathbf{R}} \tag{3.27}$$

and define H as

$$H \begin{pmatrix} \phi_1^j \\ \vdots \\ \phi_N^j \end{pmatrix} = \epsilon_j \begin{pmatrix} \phi_1^j \\ \vdots \\ \phi_N^j \end{pmatrix}. \tag{3.28}$$

H is a matrix which has diagonal elements equal to the number of nearest neighbor elements $\delta + t_{\mathbf{R}}$. For the elements H_{ij} where i and j are nearest neighbors, H_{ij} is -1. $\mathbf{T}_x$,$\mathbf{T}_y$ and $\mathbf{T}_z$ are sparse matrices whose elements are 0, 1 and -1. $t_{\mathbf{R}}$, ϵ_j and ν are dimensionless numbers. For the calculation of the scaling function, everthing is dimensionless.

Now consider the timing of our program. The matrices have $N \times N$ elements, therefore the time spent in step 1 is proportional to N^2. In step 3, the time spent in multiplying matrices of size N^2 is proportional to N^3. Considering the quick increase of running time of the matrix diagonization in step 2, the program is more time consuming with the increase of N.

On the other hand, the number of lattice sites N is related to the precison of the program. In Chapter 2, we calculated the scaling functions in the large N limit. If N is small, we are only summing over a few k points in the first Brillouin zone, which can hardly represent the real system. Therefore we have to compromise between precision and efficiency.

We test our program by calculating the scaling functions for a uniform system. We use a two-dimensional lattice for different N values. For small N our results agree with the result calculated in Chapter 2 (equation (2.44)), but deviates from the large

N limit results (2.45). As N increases, the results approaches (2.45). For a 30×30 lattice, the scaling functions agree with the results for the large N limit within 3 digits after the decimal point. So we are going to use the $N = 30 \times 30$ in the following calculation.

3.2.2 The Eigenvalue Equation

Consider the eigenvalue equation (3.27). If there is no disorder, the "eigenfunctions" are plane waves and the "eigenvalues" of H are the "energy" of the plane waves plus t. All of the eigenvalues are positive for if t is positive (which is true in our problem where $T > T_c$). If we put ramdomness into H, how will the system behave? To answer this question we have to look at the eigenvalues and eigenvectors of H first.

If we define

$$H' = H - t \cdot I, \tag{3.29}$$

then the eigenvectors $\{\phi^j_{\mathbf{R}}\}$ of H are also the eigenvectors of H', and the eigenvalues satisfy

$$\epsilon'_j + t = \epsilon_j. \tag{3.30}$$

For a given configuration of $\delta t_{\mathbf{R}}$, if we diagonalize H' then we can get the eigenvalues and eigenvectors of H at different t values.

Assume disorder is randomly distributed with a Gaussian probability function:

$$P(\delta t_{\mathbf{R}}) = \frac{1}{p\sqrt{2\pi}} e^{-(\delta t_{\mathbf{R}})^2/2p^2}, \tag{3.31}$$

where the standard deviation p denotes the strength of disorder.

We calculate the eigenvalues and eigenvectors of H' at different disorder configurations. We find that when disorder is put into the system, negative eigenvalues of H' appear. At a certain strength p, for different disorder configurations the result varies, but if we average over a large number of disorder configuration, the eigenvalues are regularly related to disorder strength p.

For 1000 disorder configurations at a certain strength p, the eigenvalues of H' are calculated. We plot the lowest eigenvalue ϵ_0' in fig. 3.1.

For the matrix H, the lowest eigenvalue $\epsilon_0 = \epsilon_0' + t$. When the temperature is close to T_c (t is small) and disorder is strong, it is possible that ϵ_0 is negative. Physically the negative eigenvalue represents the superconducting state of the system. How does the superconducting state appear when $T > T_c$? Griffiths [16] pointed out that for a large system with randomness, locally ordered regions may appear while the whole system is still in the disordered state. These rare regions lead to nonanalytical behavior of the system near T_c.

Our model in the last chapter and this chapter is based on the Ginzburg-Landau free energy for $T > T_c$. For the superconducting regions we have to consider the $|\psi|^4$ term of the free energy, and the equilibrium value of ψ is not zero. We will restrict our following discussion in the case $\epsilon_j > 0$, where no superconducting region is present.

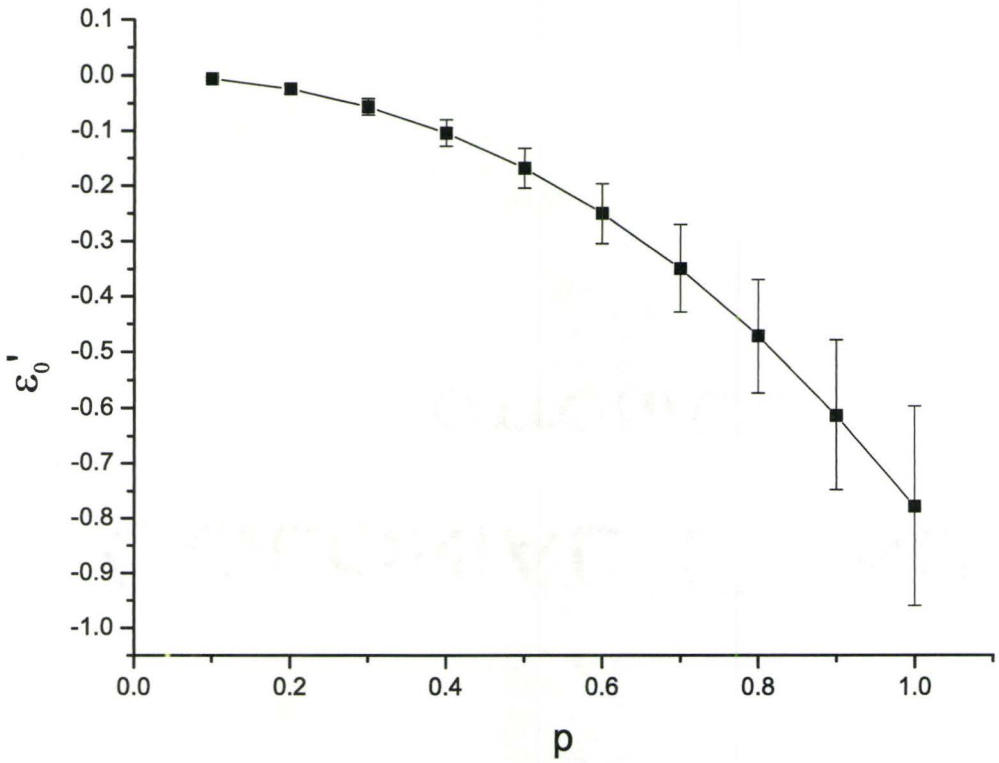

Figure 3.1: The lowest eigenvalue ϵ_0' of H' at $p = 0.1, 0.2, \cdots, 1$. The dots are the mean value of ϵ_0' and the bars are the statistical standand deviation for the 1000 disorder configurations.

3.2.3 Conductivity at Weak Disorder

We calculate the scaling functions for $p = 0.1$ and $p = 0.2$. For a two-dimensional 30×30 lattice, at a given p value 1000 different disorder configurations are averaged. The scaling functions are plotted in fig. 3.2 and fig. 3.3. To compare with the results without disorder in Chapter2 (fig. 2.1), the same set of parameters $t = 0.1, 0.2, \cdots, 1$ is chosen.

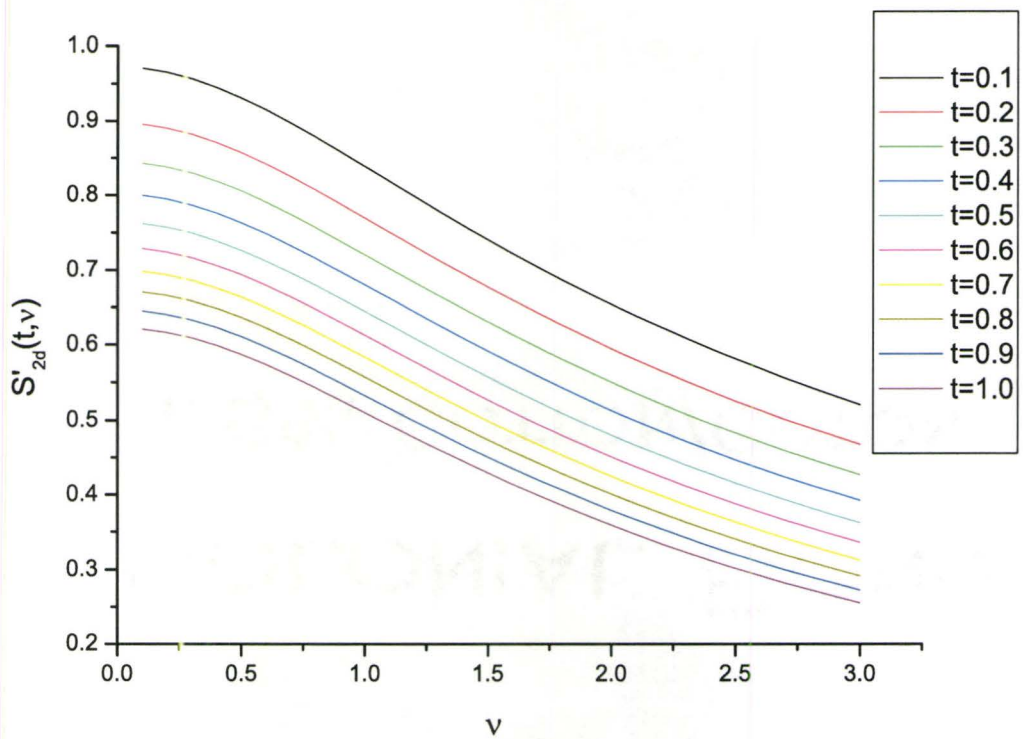

Figure 3.2: Scaling functions $S'(t, \nu)$ plotted at $p = 0.1$, $t = 0.1, 0.2, \cdots, 1$.

We plot the scaling functions with and without disorder in fig. 3.4, fig. 3.5 and

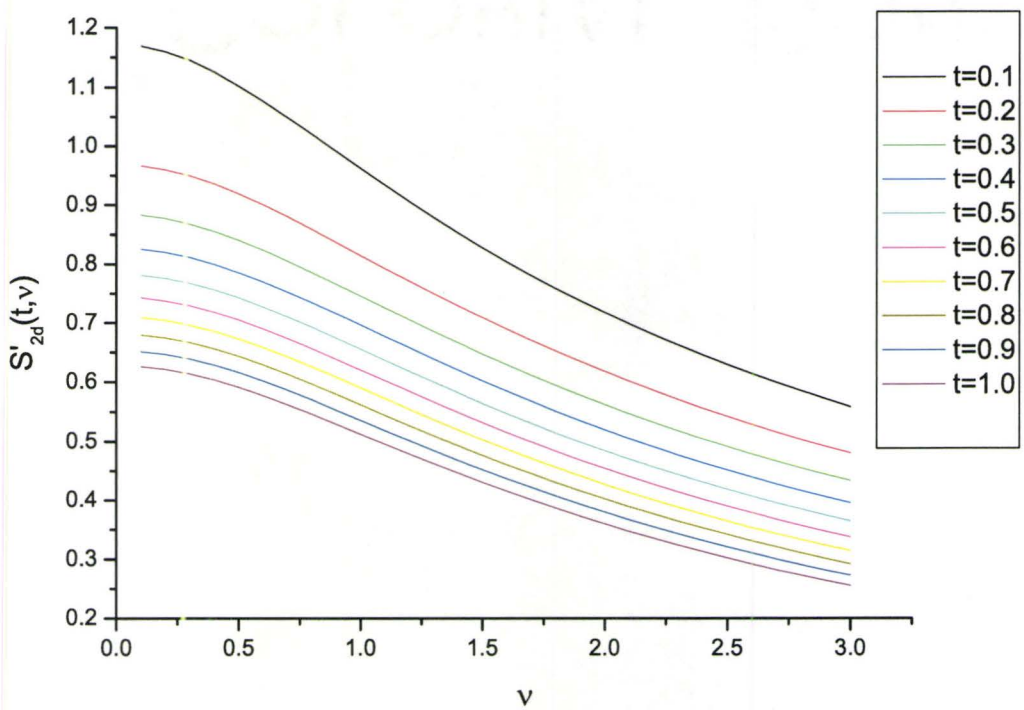

Figure 3.3: Scaling functions $S'(t, \nu)$ plotted at $p = 0.2$, $t = 0.1, 0.2, \cdots, 1$.

fig. 3.6. At the same t and ν values, the value of $S'(t,\nu)$ with disorder are larger than the clean system. At smaller t values (fig. 3.4 and fig. 3.5) this effect is stronger. At large t the curves with and without disorder almost overlap (fig. 3.6), which means that when T is far enough above T_c, disorder effects are not important to the scaling properties.

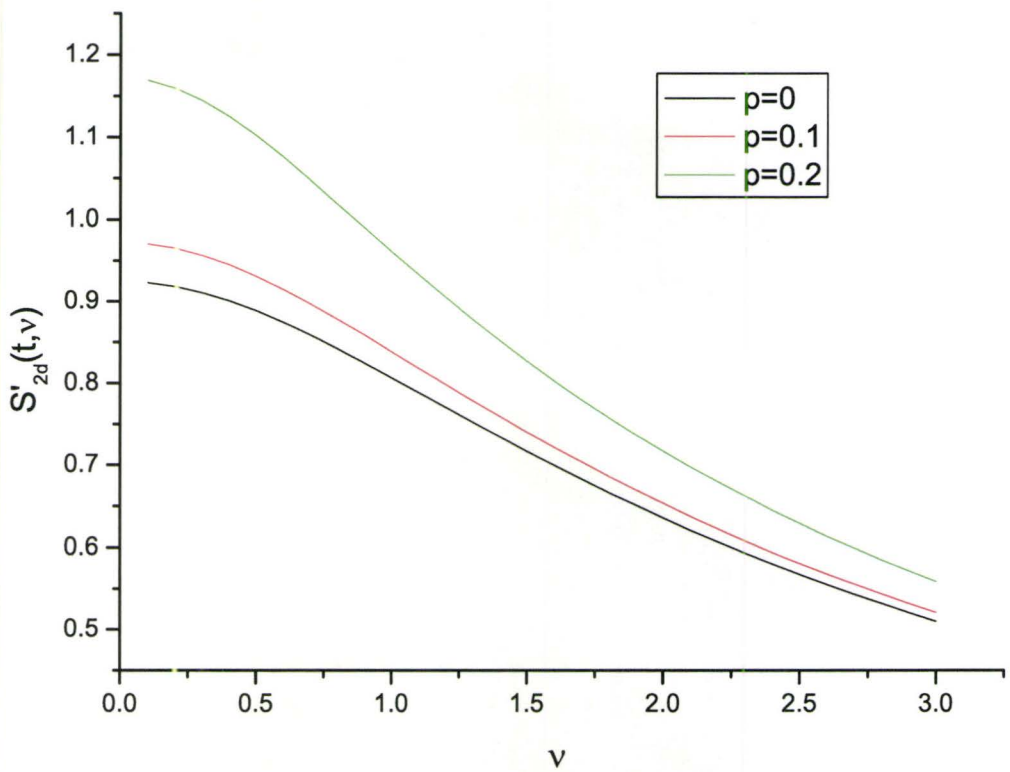

Figure 3.4: Comparison of scaling functions $S'(t,\nu)$ for $p = 0.1$, $p = 0.2$ and $p = 0$(no disorder), plotted at $t = 0.1$.

At every local lattice site, the critical temperature $T_c'(\mathbf{R})$ is randomly distributed and has equal probability to be above or below T_c', the critical temperature for the

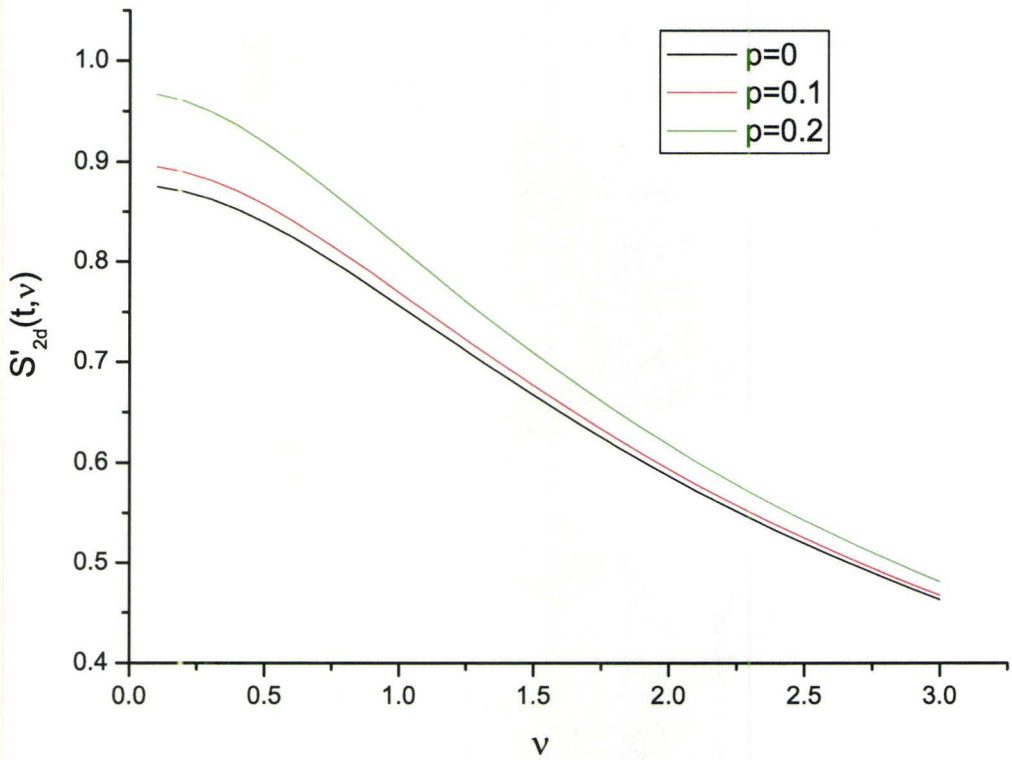

Figure 3.5: Comparison of scaling functions $S'(t, \nu)$ for $p = 0.1$, $p = 0.2$ and $p = 0$(no disorder), plotted at $t = 0.2$.

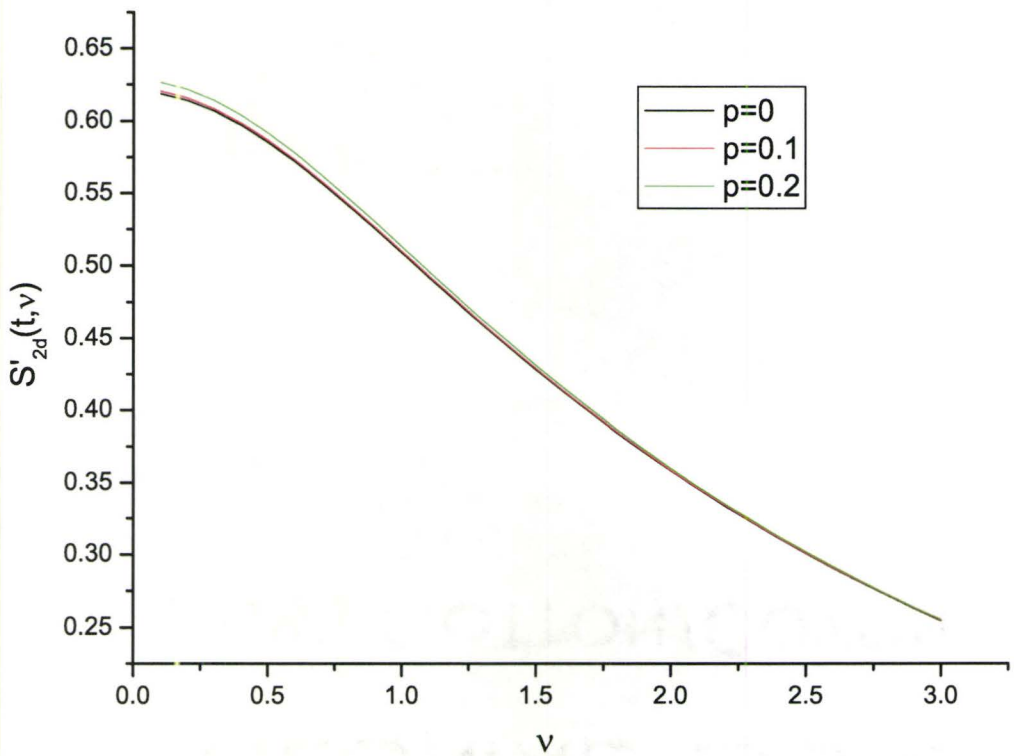

Figure 3.6: Comparison of scaling functions $S'(t, \nu)$ for $p = 0.1$, $p = 0.2$ and $p = 0$(no disorder), plotted at $t = 1.0$.

bulk system. It is interesting that the overall effect of the random distribution is to increase $S'(t, \nu)$.

Our comparison of the scaling functions with and without disorder is under the same parameter t. We didn't include the effect that disorder will change both the local critical temperature T_c and the local correlation length ξ. In a real system, disorder may preferentially lower the critical temperature and shorten the correlation length, which must be taken into account for the measured quantities in experiments.

3.2.4 Further Discussion

For the moment we have discussed the weak-disorder case under which a sharp phase transition exists. If disorder is strong enough, ϵ_0 is negative and if we continue to calculate the scaling functions, the shape of the curve is completely destroyed.

If a system has impurities that fluctuate strongly in space, the behavior near the phase transiton is often dominated by rare events, which can be described by the following physical picture:

The critical temperature of a disordered system T_c is smaller than the critical temperature of the clean system, T_{c0}. At temperature $T_c < T < T_{c0}$, the bulk system is in the disordered state, but there is a nonzero probability to find a region without impurity for an infinite size system. Local order can emerge in such regions while the bulk system is still in the disordered state. Such Griffths behavior has been studied theoretically and observed in magnetic systems.

For a superconductor the problem is more complicated. If the superconducting regions are small islands isolated by normal regions, there is no supercurrent for the bulk system. But if the superconducting regions are close to each other, they may be coupled and Josephson effects appear. These effects will bring interesting phenomena to our model, and we expect to do in-depth investigations in the future.

Chapter 4

Conclusion and Future Work

In this thesis, we investigated the effects of disorder on AC fluctuation conductivity in superconductors above T_c. We set up a lattice model to describe disorder in the superconductor and calculated the two-dimensional Gaussian scaling functions at weak disorder. The results showed that disorder will change the shape of the scaling functions, espetially at T close to T_c and low frequencies.

More work is required to reach a satisfactory explanation of fluctuation effects in high-T_c superconductors.

1. If the strength of disorder increases, it is possible that the phase transition will be smeared. We will improve our model to calculate the conductivity at strong disorder.

2. All our work so far is based on the $T > T_c$ phase where the equilibrium value of the order parameter ψ is zero. To get a complete curve of the fluctuation

peak, the conductivity below T_c must be investigated.

3. We have set up the models for two-dimensional and three-dimensional superconductors. However due to the large amount of computer time required we have only presented results for two-dimensional model in this thesis. To generalize our results for the three-dimensional systems, we are going to look for a method to diagonalize large matrices more efficiently.

4. In previous study of the fluctuation effects in superconductors near T_c, there has been a inconsistency between the theoretical and experimental value of the dynamic exponent, z. In Gaussian theory $z = 2$, while in the 3d-xy relaxtional model $z = 2.15$. Estimation from expemential data yields higher values of $z = 2.65$ [11]. We are going to examine whether disorder accounts for the discrepancy between theoretical and experimental values of the critical exponents.

Bibliography

[1] R. A. Wickham and A. T. Dorsey, Phy. Rev. B **43**, 130 (1991).

[2] D.-N. Peligrad and M. Mehring, Phys. Rev. B. **67**, 174515 (2003).

[3] M. Tinkham, *Introduction to Superconductivity*, 2nd ed. (McGraw-Hill, New York, 1996).

[4] W. J. Skocpol and M. Tinkham, Rep. Prog. Phys. **38**, 1049 (1975).

[5] H. Schmidt, Z. Physik **216**, 336 (1968).

[6] H. Schmidt, Z. Physik **232**, 443 (1970).

[7] D. A. Bonn and W. N. Hardy, Physics in Canada **56**, 243 (2000).

[8] S. Kamal *et al.*, Phys. Rev. Lett. **73**, 1845 (1994).

[9] W. N. Hardy, D. A. Bonn, R. Liang, and S. Kamal (unpublished).

[10] R. E. Glover, Phys. Lett. **25A**, 542 (1967).

[11] J. C. Booth *et al.*, Phys. Rev. Lett. **77**, 4438 (1996).

[12] D. S. Fisher, M. P. A. Fisher, and D. A. Huse, Phy. Rev. B **43**, 130 (1991).

[13] A. B. Harris, J. Phys. C **7**, 1671 (1974).

[14] T. Vojta and R. Sknepnek, Phys. Stat. Sol. (b) **241**, 2118 (2004).

[15] N. Goldenfeld, *Lectures on Phase Transitions and the Renormalization Group* (Addison-Wesley, Reading, Massachusetts, 1992).

[16] R. B. Griffiths, Phys. Rev. Lett. **23**, 17 (1969).